Two competing pathways of aerosol effects on cloud and precipitation formation

Toshihiko Takemura,[1] Yoram J. Kaufman,[2,3] Lorraine A. Remer,[2] and Teruyuki Nakajima[4]

Received 2 October 2006; revised 14 November 2006; accepted 9 January 2007; published 17 February 2007.

[1] Aerosols may influence cloud formation through two pathways: One is the effect on cloud microphysics by forming smaller and more numerous cloud droplets reducing precipitation and consequently enhancing cloud lifetime. The second is referred to as the aerosol dynamic-hydrological effect in which the aerosol direct, semi-direct, and indirect effects can modulate atmospheric radiation, which perturbs atmospheric circulation, leading to redistributions of clouds and precipitation. Here this study examines climate sensitivities using a general circulation model coupled with an aerosol transport-radiation model. The model is run first with prescribed meteorology in order to isolate the cloud microphysical effect. It is run in a separate experiment with internally generated meteorology that includes dynamic-hydrological effect as the aerosols modify clouds and interact with the radiation. We find in some regions that the dynamic-hydrological effect in the free model runs counteracts the microphysical effects seen in the prescribed runs. **Citation:** Takemura, T., Y. J. Kaufman, L. A. Remer, and T. Nakajima (2007), Two competing pathways of aerosol effects on cloud and precipitation formation, *Geophys. Res. Lett.*, *34*, L04802, doi:10.1029/2006GL028349.

1. Introduction

[2] Aerosol particles, suspended particle matter in the atmosphere, not only may have harmful influence on human health but also may lead to climate change through several processes. The aerosol direct effect is a change in the atmospheric radiation budget caused by scattering and absorption by aerosol particles [*Charlson et al.*, 1992]. In the aerosol semi-direct effect, radiative absorption by aerosols heats the surrounding atmosphere, and consequently causes atmospheric stratification, leading to reduction of cloud cover [*Hansen et al.*, 1997; *Koren et al.*, 2004]. The most uncertain processes are the first and second indirect effects. In the first indirect effect an increase in aerosol concentration acting as cloud condensation nuclei (CCN) results in smaller and more numerous cloud droplets if the liquid water content is constant, which leads to higher cloud reflectance [*Twomey et al.*, 1984]. In the second indirect effect a decrease in the cloud droplet size causes an inhibition of precipitation, and consequently increases the cloud lifetime [*Albrecht*, 1989]. The Third Assessment Report of the Intergovernmental Panel on Climate Change (IPCC TAR) estimated the radiative forcing from the pre-industrial era to the present. The estimate indicated a large uncertainty with a change in the atmospheric radiation budget due to aerosols to be in a wide range of 0 to -2 W m^{-2} without suggesting an average value for the first indirect effect, and it refrained from an estimation of the second indirect effect because there were few observational and modeling studies [*Intergovernmental Panel on Climate Change* (*IPCC*), 2001]. After IPCC TAR, further studies on the aerosol indirect effect have begun using in-situ and satellite observations and modeling simulations [e.g., *Nakajima et al.*, 2001; *Lohmann and Lesins*, 2002]. Cloud formation largely depends not only on the cloud microphysical process that occurs on the scale of individual cloud lifetimes, but also on changes in the dynamic and hydrological fields triggered by, for example, variations of the atmospheric radiation and phases of water that evolve over a wide variety of time scales. Clouds are one of the most important factors in regulating meteorological and climatic conditions through the radiation budget and forming precipitation.

[3] Recent analysis of Moderate Resolution Imaging Spectroradiometer (MODIS) data showed large increases in the cloud fraction with an increase in the aerosol optical thickness, corresponding to the aerosol indirect forcing of -5 to -10 W m^{-2} over the Northern Atlantic Ocean in the boreal summer [*Kaufman et al.*, 2005; *Koren et al.*, 2005]. It is, however, technically difficult for these measurements to separate the feedback processes of the aerosol-cloud-climate interaction from the total aerosol effects because the real climate includes all of various microphysical and feedback mechanisms. There were also some past studies in which the feedback mechanisms with the aerosol effects were discussed using general circulation models [e.g., *Quaas et al.*, 2004; *Hansen et al.*, 2005]. These modeling studies, however, did not clearly discuss separation of the microphysical effects from the feedback effects. Here, in this study, we show simulated liquid water path and precipitation both with and without the feedback mechanism using a global aerosol transport-radiation model, SPRINTARS.

2. Method

[4] SPRINTARS is coupled with an atmospheric general circulation model (AGCM) from the Center for Climate System Research (CCSR), University of Tokyo/National Institute for Environmental Studies (NIES)/Frontier Research Center for Global Change (FRCGC) [*K-1 Model Developers*, 2004]. The AGCM can be coupled to a mixed layer ocean model. A simulation without the mixed layer ocean needs prescribed data of sea surface temperature

[1]Research Institute for Applied Mechanics, Kyushu University, Fukuoka, Japan.
[2]NASA Goddard Space Flight Center, Greenbelt, Maryland, USA.
[3]Deceased 31 May 2006.
[4]Center for Climate System Research, University of Tokyo, Chiba, Japan.

0094-8276/07/2006GL028349$05.00

(SST) and sea ice, and therefore cannot include the interaction between the atmospheric field and SST/sea ice. On the other hand, a simulation with the mixed layer ocean accounts for the feedback mechanism between the atmosphere and SST/sea ice. In this study, the horizontal resolution of the triangular truncation is set at T42 (approximately 2.8° by 2.8° in longitude and latitude) and the vertical resolution at 20 layers with the standard time step of 20 minutes. SPRINTARS treats the transport processes of the main tropospheric aerosols of black carbon, organics, sulfate, soil dust, and sea salt, originating both from natural and anthropogenic sources. These aerosol fields interact with the radiation processes of the AGCM. SPRINTARS includes a microphysical parameterization of the cloud-aerosol interaction based on the Köhler theory [*Abdul-Razzak and Ghan*, 2000], so that water clouds and grid-scale precipitation depend on the particle number concentrations, size distributions, and chemical properties for each aerosol species. The simulated cloud droplet effective radius, cloud radiative forcing, and precipitation are confirmed to be in reasonable agreement with observations [*Takemura et al.*, 2005]. The detailed descriptions of SPRINTARS are in the work of *Takemura et al.* [2000, 2002, 2005]. The research field analyzed in this study is the Atlantic region, similar to the satellite-based studies of *Kaufman et al.* [2005] and *Koren et al.* [2005]. Over this region a large amount of aerosols exist originating from human urban/industrial pollution in mid-latitudes of the Northern Hemisphere, biomass burning in the sub-tropics of the Southern Hemisphere and tropics, and Saharan dust. In this region, 68% of cloud mass is in the liquid phase and the other is in the ice phase. In the model, microphysical cloud-aerosol interaction takes place only in the liquid phase [*Takemura et al.*, 2005].

[5] Here SPRINTARS with the mixed-layer ocean simulates three different scenarios of aerosol emissions and greenhouse gas (GHG) concentrations in order to analyze the aerosol effects on climate: present aerosols and present GHGs experiment (E1), pre-industrial aerosols and present GHGs experiment (E2), and pre-industrial aerosols and pre-industrial GHGs experiment (E3). The difference between E1 and E2 (E1−E2) is due to a change in aerosols only, while E1−E3 is due to a change both in aerosols and GHGs. Each equilibrium experiment is integrated for fifty years and analyzed for the last thirty years to exclude the impact of initial inequilibrium conditions. Concentrations for GHGs and emission fluxes for anthropogenic aerosols in the pre-industrial era and present day are provided from *Johns et al.* [2003] and CCSR/NIES/FRCGC [*Nozawa et al.*, 2005], respectively. Each experiment consists of three ensemble simulations starting from different initial conditions, which are in the first day of different years from the control run of the CCSR/NIES/FRCGC atmosphere-ocean general circulation model [*Nozawa et al.*, 2005], to reduce uncertainties of simulations.

[6] Experiments E1 and E2 are repeated as E1f and E2f respectively, for prescribed winds, atmospheric temperature, and specific humidity by 6-hourly NCEP/NCAR reanalysis data from the years 1997 to 2002 as well as prescribed sea surface temperature and sea ice to exclude any feedbacks due to the aerosol effects. E1f and E2f are analyzed for the last five years. Their meteorological parameters are matched at each time step to the reanalysis field, though the wind and temperature are not controlled below the vertical sigma level of 0.9 because of preventing calculation instability. The present model re-diagnoses cloud water from total water, that is specific humidity plus cloud water, in the cloud-precipitation process at each time step with the saturation scheme. After the diagnosis, a portion of cloud water converts to precipitation with the aerosol second indirect effect according to the Berry's parameterization [*Takemura et al.*, 2005, equation (6)]. Therefore by controlling the specific humidity and holding it to observed conditions in the short term integrations (E1f and E2f) the dynamic-hydrological feedbacks are almost removed. This allows us to isolate the aerosol effect on cloud microphysics.

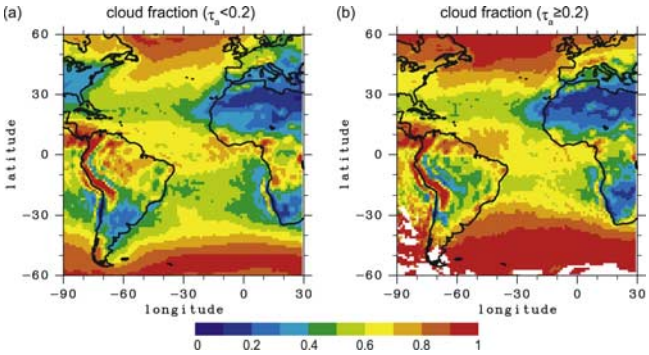

Figure 1. Annual mean distributions of the simulated cloud fraction in the simulated aerosol optical thickness: (a) less than 0.2 and (b) above 0.2. Daily mean data are sorted by the aerosol optical thickness and then averaged. The simulation is prescribed by 6-hourly NCEP/NCER reanalysis data for wind, temperature, and specific humidity from 1998 to 2002.

3. Results and Discussion

[7] Figure 1 shows present-day conditions (E1f) of the simulated cloud fraction classified by the simulated aerosol optical thickness less than and above 0.2 with the prescribed meteorological field. It is handled by the same statistical method as the MODIS analysis in the work of *Koren et al.* [2005, Figure 1]. In the MODIS analysis, the cloud fraction and water cloud optical thickness increase with increasing aerosol optical thickness in all latitudes over the Atlantic Ocean in the Northern Hemisphere [*Koren et al.*, 2005], while the simulation in the Figure 1 indicates a significant increase in the cloud fraction only in the eastern North America and north of 40°N. The difference between the MODIS analysis and the model simulation suggests that the model may be missing some aerosol-cloud processes. It seems to capture the interaction correctly when hygroscopic anthropogenic aerosols are involved, but misses in areas with natural dust particles. Missing the process of cloud interaction with natural dust should not affect the results when we compare present-day to pre-industrial aerosol conditions because a difference in the aerosol loading between the two conditions is almost due to anthropogenic aerosols (see Figure 2b).

[8] To demonstrate the effects of anthropogenic aerosols on the cloud field in more detail, we show the differences

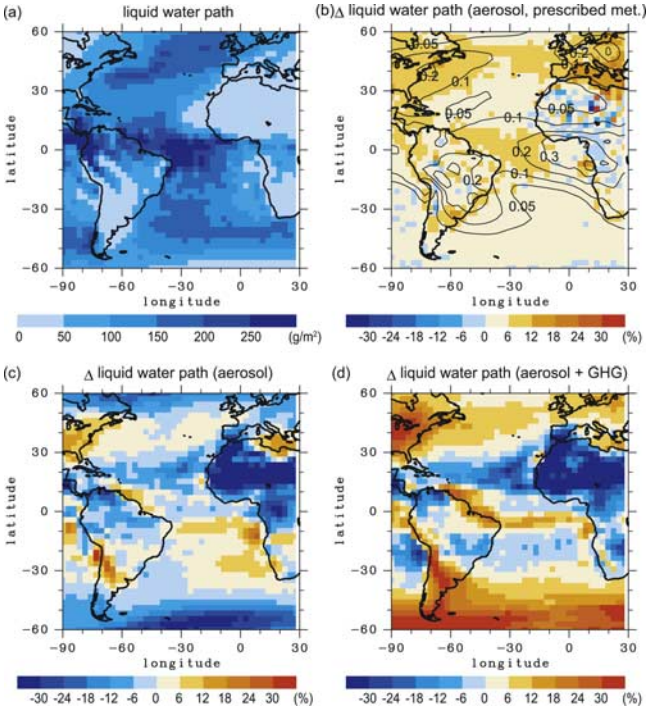

Figure 2. (a) Annual mean distributions of the simulated liquid water path and (b) its changes from the pre-industrial era to the present with changes in aerosols with prescribed meteorological field (difference between the experiments E1f and E2f), (c) aerosols without restrictions on the meteorological fields including feedback (difference between E1 and E2), and (d) both aerosols and GHGs without restrictions on the meteorological fields including feedback (difference between E1 and E3). Contours in Figure 2b indicate a difference in the annual mean aerosol optical thickness between the pre-industrial era and the present day. Their intervals are 0.05, 0.1, 0.2, 0.3, and 0.4.

among scenarios E1, E2, E3, E1f, and E2f in Figure 2. Figure 2a shows the annual mean liquid water path in E1f, and there are no significant differences in the liquid water path between E1f and E1 (not shown). The impact of anthropogenic aerosols on cloud formation for the prescribed meteorological field is shown in Figure 2b (E1f–E2f). The drawn black contour lines show the increase in aerosol optical thickness from pre-industrial to present days. The colors show the cloud response in terms of liquid water path. The annual mean aerosol optical thickness over the Atlantic Ocean between 60°N and 60°S increases by 100% and the annual mean liquid water path increases by 5% as compared with pre-industrial conditions. Over the Atlantic Ocean the increases in anthropogenic aerosols are concentrated downwind of biomass burning regions and in the northern mid-latitudes where pollution from urban/industrial activities is located. The increase in the liquid water path due to the longer cloud lifetime is significant where we see both an increase in anthropogenic aerosols and sufficient liquid water path. This appears not only as a continuous band from continental North America, across the ocean to Europe where urban/industrial aerosol dominates, but also over the open ocean in the biomass-burning aerosol region. Over the continents and near the African coast, the aerosol-induced increase in liquid water path is negligible. The liquid water path is slightly decreased over the African continent because the wind and temperature are not prescribed near the surface as mentioned in the previous section. Therefore the strong heating near the surface creates a dynamical difference between E1f and E2f, which consequently suppresses the liquid water path.

[9] Relaxing the restrictions on the meteorological field and sea surface temperature allows the system to adjust to aerosol dynamic-hydrological effects. For example, the direct and indirect effects will cause less insolation at the surface and result in a decrease of evaporation and heat fluxes. These will lead to a decrease in available water vapor for cloud formation and an expected decrease in liquid water path, as well as changing the atmospheric circulation. The semi-direct effect due to radiative-absorbing aerosols can modulate atmospheric heating, also leading to changes in liquid water path and atmospheric circulation. As expected, permitting adjustment of the meteorological field in the model reverses the effect on changing the liquid water path from positive to negative in some regions (Figure 2c) (E1–E2). The liquid water path is still increased in the mid-latitudes of the Northern Hemisphere and the sub-tropics of the Southern Hemisphere where anthropogenic aerosols dominate. A difference between Figures 2b and 2c suggests that the aerosol dynamic-hydrological effect is significant in determining the large-scale impact of aerosols on cloud fields. With the feedback mechanism including both anthropogenic aerosols and GHGs (Figure 2d) (E1–E3), the liquid water path is increased in mid- and high-latitudes of both Hemispheres, while the decrease is reinforced in the sub-tropics of the Northern Hemisphere.

[10] Figure 3 summarizes changes in the liquid water path over the Atlantic Ocean. Figure 3 clearly shows that the aerosol microphysical effect (dashed line) increases the liquid water path especially in the Northern Hemisphere because of the high concentrations of anthropogenic aerosols. Figure 3 also indicates that the change in the liquid water path with the feedback mechanism (dotted line) is much different from the experiment with only the micro-

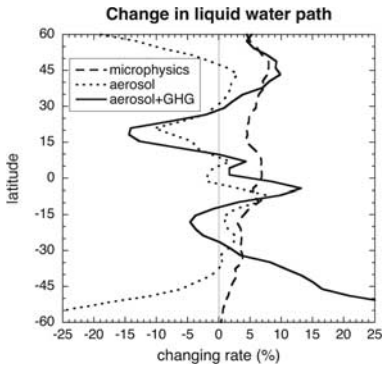

Figure 3. Zonal mean changing rates in the simulated liquid water path from the pre-industrial era to the present by the aerosol microphysical effect (dashed line, difference between the experiments E1f and E2f), aerosol microphysical plus dynamic-hydrological effects (dotted line, difference between E1 and E2), and all of aerosol plus GHG effects (solid line, difference between E1 and E3) over the Atlantic Ocean.

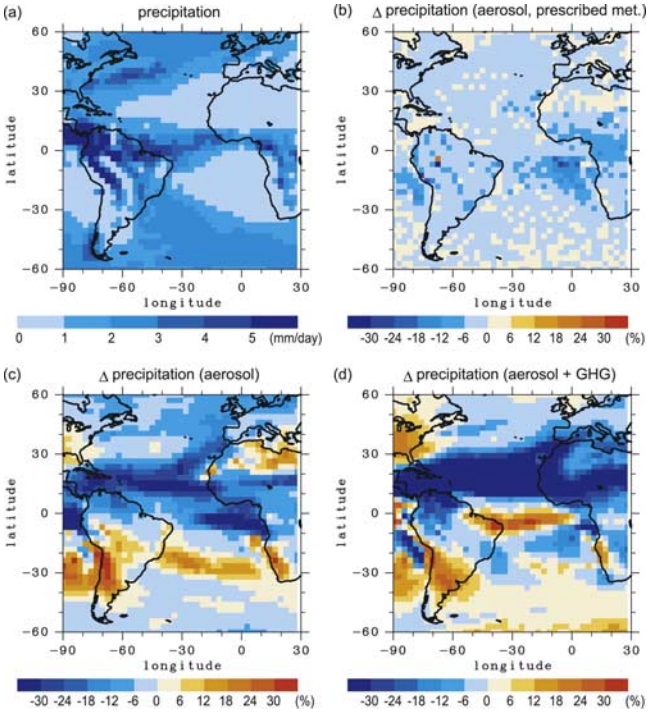

Figure 4. Same as Figure 2 but for the simulated precipitation.

physical effect. Another interesting point is that the difference in the liquid water path between the total aerosol effect (dotted line) and the aerosol plus GHG effect (solid line) shows a shift of the Intertropical Convergence Zone (ITCZ) due to anthropogenic aerosols, which was discussed by *Rotstayn and Lohmann* [2002] and *Takemura et al.* [2005].

[11] The smaller cloud droplets correspond to less grid-scale precipitation for a given cloud water content in the parameterization of the aerosol second indirect effect [*Takemura et al.*, 2005, equation (6)]. The simulation shows that anthropogenic aerosols suppress the precipitation over the tropics and sub-tropics because of the microphysical effect on liquid water, though there is little increase in other regions because much of the precipitation in mid- and high-latitudes includes cold cloud processes, which the model does not parameterize (Figure 4b) (E1f–E2f). Relaxation of the restriction on the meteorological field results in a decrease (increases) in the precipitation corresponding to a decrease (increase) in the liquid water path over much of the Atlantic region (Figure 4c) (E1–E2). This positive correlation between precipitation and liquid water path is contrary to our expectations from the aerosol second indirect effect. Dynamics must be dominating these conditions. However E1–E2 indicates an increase in the liquid water path (Figure 2c) and a decrease in the precipitation (Figure 4c) over the North Atlantic Ocean between 30° and 45°N where there is an outflow region of anthropogenic aerosols from human urban/industrial activities in the United States. The simultaneous change of the increase in the liquid water path and the decrease in the precipitation suggests the aerosol second indirect effect dominates when hygroscopic pollution particles are prevalent. A large difference between Figures 4b and 4c suggests that the aerosol dynamic-hydrological effect for the precipitation is significant.

[12] The simulated precipitation both with anthropogenic aerosols and GHGs (Figure 4d) (E1–E3) can be compared with historical observational data. The observed trend of a change in the annual precipitation in the 20th century reveals a decrease of several tens of percent in the Sahel and central Africa and an increase in most areas of the North America [*IPCC*, 2001]. These trends are simulated well in the model, and a comparison between Figures 4c and 4d indicates that the aerosol effect contributes to these precipitation changes from the pre-industrial era to the present day. The simulation suggests that anthropogenic aerosols accelerate drought in the Sahel through the feedback mechanism [*Rotstayn and Lohmann*, 2002].

4. Summary

[13] We performed simulations to analyze both the aerosol microphysical and dynamic-hydrological effects on clouds and precipitation by a global aerosol transport-radiation model. We used prescribed meteorological fields to isolate the aerosol effect on the cloud microphysics. Then, we excluded these restrictions by coupled with a mixed-layer ocean model, which included aerosol dynamic-hydrological effects such as reduced surface insolation resulting in reduced evaporation, i.e., the feedback mechanism. The experiments clearly indicate that the simulated aerosol effect on liquid water and precipitation are very different depending on whether the feedback mechanism is permitted in the model. Similar experimental sets to this study but including the aerosol-ice cloud interaction will be useful in understanding additional microphysical and feedback mechanisms of the anthropogenic aerosol effects on climate change.

[14] **Acknowledgments.** We thank the contributors to development of SPRINTARS and CCSR/NIES/FRCGC GCM, NIES and Fujitsu FIP Corporation for providing emission data related to aerosols, NOAA-CIRES Climate Diagnostics Center for providing NCEP/NCAR reanalysis data, Hongbin Yu for useful comments, and reviewers. SPRINTARS simulates on NEC SX-6 of NIES. This study is supported by the Visiting Fellow Program of Goddard Earth Sciences and Technology Center (GEST)/ University of Maryland Baltimore County (UMBC) and NASA Goddard Space Flight Center, and the Special Coordination Funds for Promoting Science and Technology and the Grand-in-Aid for Young Scientists of the Ministry of Education, Culture, Sports, Science, and Technology of Japan. This is one of the last studies of Yoram J. Kaufman before he passed away in a contingent traffic accident. This paper is dedicated to him.

References

Abdul-Razzak, H., and S. J. Ghan (2000), A parameterization of aerosol activation: 2. Multiple aerosol types, *J. Geophys. Res.*, *105*, 6837–6844.

Albrecht, B. A. (1989), Aerosols, cloud microphysics, and fractional cloudiness, *Science*, *245*, 1227–1230.

Charlson, R. J., S. E. Schwartz, J. M. Hales, R. D. Cess, J. A. Coakley Jr., J. E. Hansen, and D. J. Hofmann (1992), Climate forcing by anthropogenic aerosols, *Science*, *255*, 423–430.

Hansen, J., M. Sato, and R. Ruedy (1997), Radiative forcing and climate response, *J. Geophys. Res.*, *102*, 6831–6864.

Hansen, J., et al. (2005), Earth's energy imbalance: Confirmation and implications, *Science*, *308*, 1431–1435.

Intergovernmental Panel on Climate Change (IPCC) (2001), *Climate Change 2001: The Scientific Basis: Contribution of Working Group I to the Third Assessment Report of the Intergovernmental Panel on Climate Change*, edited by J. T. Houghton et al., 881 pp., Cambridge Univ. Press, New York.

Johns, T. C., et al. (2003), Anthropogenic climate change for 1860 to 2100 simulated with the HadCM3 model under updated emissions scenarios, *Clim. Dyn.*, *20*, 583–612.

K-1 Model Developers (2004), K-1 coupled GCM (MIROC) description, edited by H. Hasumi and S. Emori, *K-1 Tech. Rep. 1*, 34 pp., Cent. for Clim. Syst. Res., Univ. of Tokyo, Tokyo.

Kaufman, Y. J., I. Koren, L. A. Remer, D. Rosenfeld, and Y. Rudich (2005), The effect of smoke, dust, and pollution aerosol on shallow cloud development over the Atlantic Ocean, *Proc. Natl. Acad. Sci. U. S. A.*, *102*, 11,207–11,212.

Koren, I., Y. J. Kaufman, L. A. Remer, and J. V. Martins (2004), Measurement of the effect of Amazon smoke on inhibition of cloud formation, *Science*, *303*, 1342–1345.

Koren, I., Y. J. Kaufman, D. Rosenfeld, L. A. Remer, and Y. Rudich (2005), Aerosol invigoration and restructuring of Atlantic convective clouds, *Geophys. Res. Lett.*, *32*, L14828, doi:10.1029/2005GL023187.

Lohmann, U., and G. Lesins (2002), Stronger constraints on the anthropogenic indirect aerosol effect, *Science*, *298*, 1012–1015.

Nakajima, T., A. Higurashi, K. Kawamoto, and J. E. Penner (2001), A possible correlation between satellite-derived cloud and aerosol microphysical parameters, *Geophys. Res. Lett.*, *28*, 1171–1174.

Nozawa, T., T. Nagashima, H. Shiogama, and S. A. Crooks (2005), Detecting natural influence on surface air temperature change in the early twentieth century, *Geophys. Res. Lett.*, *32*, L20719, doi:10.1029/2005GL023540.

Quaas, J., O. Boucher, J.-L. Dufresne, and H. L. Treut (2004), Impacts of greenhouse gases and aerosol direct and indirect effects on clouds and radiation in atmospheric GCM simulations of the 1930–1989 period, *Clim. Dyn.*, *23*, 779–789.

Rotstayn, L. D., and U. Lohmann (2002), Tropical rainfall trends and the indirect aerosol effect, *J. Clim.*, *15*, 2103–2116.

Takemura, T., H. Okamoto, Y. Maruyama, A. Numaguti, A. Higurashi, and T. Nakajima (2000), Global three-dimensional simulation of aerosol optical thickness distribution of various origins, *J. Geophys. Res.*, *105*, 17,853–17,873.

Takemura, T., T. Nakajima, O. Dobovik, B. N. Holben, and S. Kinne (2002), Single-scattering albedo and radiative forcing of various aerosol species with a global three-dimensional model, *J. Clim.*, *15*, 333–352.

Takemura, T., T. Nozawa, S. Emori, T. Y. Nakajima, and T. Nakajima (2005), Simulation of climate response to aerosol direct and indirect effects with aerosol transport-radiation model, *J. Geophys. Res.*, *110*, D02202, doi:10.1029/2004JD005029.

Twomey, S., M. Piepgrass, and T. L. Wolfe (1984), An assessment of the impact on global cloud albedo, *Tellus, Ser. B*, *36*, 356–366.

T. Nakajima, Center for Climate System Research, University of Tokyo, 5-1-5 Kashiwanoha, Chiba 277-8568, Japan.

L. A. Remer, Laboratory for Atmospheres, NASA GSFC, Code 613.2, Greenbelt, MD 20771, USA.

T. Takemura, Research Institute for Applied Mechanics, Kyushu University, 6-1 Kasuga-kouen, Fukuoka 816-8580, Japan. (toshi@riam.kyushu-u.ac.jp)